Structure-Based Design of Glycodendrimer Antagonists for Improved DC-SIGN Targeting

Giulio Goti[1], Cinzia Colombo[1], Silvia Achilli [2,3], Corinne Vivès [2], Michel Thépaut [2], Frank Fieschi [2,*], Anna Bernardi [1,*]

[1] Università degli Studi di Milano, Dipartimento di Chimica, via Golgi 19, 20133, Milano, Italy
[2] Université Grenoble Alpes, CEA, CNRS Institut de Biologie Structurale, avenue des Martyrs 71, 38000, Grenoble, France
[2] Present address: Univ. Grenoble Alpes, CNRS, Departement de Pharmacochimie Moléculaire, 38044 Grenoble, France
* Correspondence: anna.bernardi@unimi.it

Received: date; Accepted: date; Published: date

Abstract: DC-SIGN multivalent antagonists have emerged as effective antiadhesive agents against various pathogen infections. Recently, our group have shown that high potency can be achieved upon bridging two of the four binding sites displayed by the protein. Here we present our endeavors to accomplish the tetracoordination of DC-SIGN through the synthesis of two cross-shaped glycodendrimers. The choice of a tailored rigid scaffold allowed multivalent presentation of glycomimetics in a spatially defined fashion, while providing good water solubility to the constructs. Evaluation of the biological activity by SPR assay revealed strong binding avidity towards DC-SIGN and increased selectivity over langerin.

Keywords: glycodendrimers; multivalency; glycomimetics; DC-SIGN; langerin; Surface Plasmon Resonance.

1. Introduction

Carbohydrate-protein interaction in living systems is an archetype of multivalency, where proteins (called lectins) presenting either multiple carbohydrate recognition domains (CRDs) or an oligomeric structure selectively recognize and bind to specific polyglycosylated targets [1]. This strategy takes advantage of the mechanisms governing multivalency, *i.e.* chelation, statistical rebinding and receptor clustering, to provide strong binding, while overcoming the intrinsic low affinity of the monovalent glycan ligands for their receptors [2-4].

Following the very same approach, the past two decades have seen a prosperous generation of multivalent glycoconjugate antagonists able to interfere with such interactions [5-9]. Altogether, these studies revealed the complexity in designing effective antagonists, whose efficacy is determined by the nature of the ligand displayed, as well as by parameters of difficult prediction, such as the architecture of the polyvalent scaffold, the valency, the ligand density, the kind of linker engaged and the flexibility of the construct.

Lately we have disclosed structure-based design as a guiding principle in the development of strong polyglycosylated antagonists for Dendritic Cell-Specific Intercellular adhesion molecule-3 (ICAM-3)-Grabbing Non-integrin (DC-SIGN) [10-13], a tetrameric transmembrane C-type lectin receptor (Figure 1) exploited by pathogens such as HIV, Ebola, Hepatitis C, to invade the host and propagate the infection [14,15]. While multiple ligand presentation on polyvalent scaffolds is generally the choice to achieve high avidity towards DC-SIGN [7-9], we showed that scaffold optimization plays a role in achieving high affinity levels with constructs of relatively low valency. Specifically, rigid rod-like scaffolds of controlled length were loaded with glycodendrons, giving access to hexavalent constructs (Polyman-31 **PM31** and and Polyman-26 **PM26**, depending on the monovalent ligand, Figure 2) [16] able to bridge two contiguous CRDs within the DC-SIGN tetramer, that are separated by ca. 4 nm. These constructs showed nanomolar activity in the

inhibition of DC-SIGN mediated HIV infection [11, 17], in sharp contrast with the low micromolar activity range of less preorganized structures of similar or even higher valency [18].

The strong impact of chelation on the inhibition potency led us to consider whether stronger antagonists could be obtained by simultaneous binding of the four CRDs of DC-SIGN extra-cellular domain (ECD), which are arranged at the four corners of a square with 4 nm side and a 5.5 nm diagonal (Figure 1).

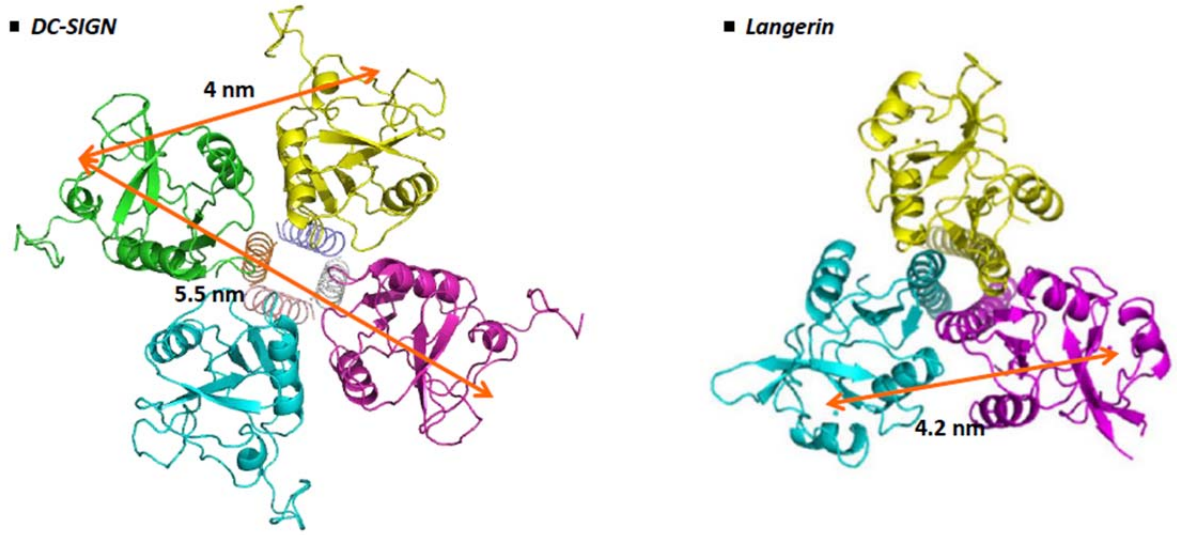

Figure 1. Crystallographic structures of the DC-SIGN ECD tetramer and langerin ECD trimer. The four CRDs of DC-SIGN are exposed at the vertexes of a squared with a diagonal distance of 5.5 nm. langerin is characterized by a trefoil structure displaying three CRDs which are spaced by 4.2 nm.

To test this hypothesis, we targeted the synthesis of cross-shaped glycodendrimers **C1,2** (Figure 2). These compounds are characterized by a tetravalent rigid core of 22 Å diagonal length, which is prolonged by four copies of trivalent glycodendron moieties, resulting in an extended distance over 6 nm between two complexing units [11]. As monovalent ligands, we selected the pseudo-disaccharide **1** and the corresponding more potent bis-*p*-hydroxymethylbenzylamide derivative **2**, which we previously reported as effective and selective DC-SIGN antagonists [10,19]. Ideally, the tailored geometry of the scaffold would confer optimal ligand presentation towards DC-SIGN, while disfavoring a-specific binding to C-type lectins characterized by a different spatial arrangement of their CRDs [20].

Herein, we report the realization of our idea through the synthesis of compounds **C1,2** and the evaluation of their interaction with DC-SIGN by Surface Plasmon Resonance (SPR). Selectivity over langerin, a trimeric C-type lectin with protective effects against HIV infection [21], was also assessed.

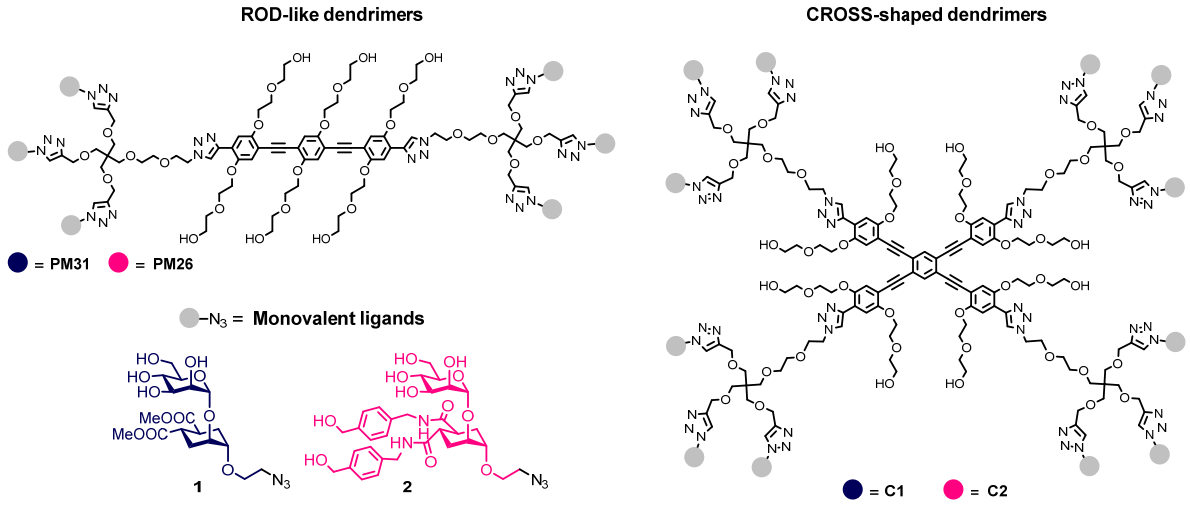

Figure 2. Structures of the previously developed rigid linear glycodendrimers **PM31**, **PM26** and of the targeted cross-shaped glycodendrimers **C1,2**. Both scaffolds are functionalized with multiple copies of either the pseudo-dimannobioside **1** or with the bis-amido derivative **2**.

2. Materials and Methods

2.1. General methods and procedures

Chemicals were purchased from commercial sources and used without further purification, unless otherwise indicated. When anhydrous conditions were required, the reactions were performed under nitrogen atmosphere. Anhydrous solvents were purchased from Sigma-Aldrich® with a content of water ≤ 0.005 %. *N,N'*-Diisopropylethylamine (DIPEA) was dried over calcium hydride, THF was dried over sodium/benzophenone and freshly distilled before use. Reactions were monitored by analytical thin-layer chromatography (TLC) performed on Silica Gel 60 F_{254} plates (Merck) with UV detection (254 nm and 365 nm) and/or staining with ammonium molybdate acid solution or potassium permanganate alkaline solution. Flash column chromatography was performed according to the method of Still and co-workers [22] using silica gel 60 (40-63 μm) (Merck). Size-exclusion chromatography was performed using Sephadex LH-20 from GE Helthcare Life Science. HPLC analyses were performed with an Atlantis T3 5 μm 4.6x100 mm column (Waters) equipped with a Waters 996 Photodiode Array Detector. NMR experiments were recorded either on a Bruker AVANCE-600 MHz or a Bruker AVANCE-400 MHz instrument at 298 K. Chemical shifts (δ) are reported in ppm. The ^{1}H and ^{13}C NMR resonances of compounds were assigned with the assistance of COSY and HSQC experiments. Multiplicities are assigned as s (singlet), d (doublet), t (triplet), quint. (quintet), m (multiplet), b (broad). EI-MS spectra were collected using a VG AUTOSPEC- M246 spectrometer (double-focusing magnetic sector instrument with EBE geometry) equipped with EI source. Solid samples were introduced via a heated direct insertion probe. ESI-MS spectra were recorded on Waters Micromass Q-TOF (ESI ionization-HRMS). MALDI-TOF MS spectra were recorded on Bruker Daltonics Microflex LT. The following abbreviations are used: CuAAC (copper catalyzed azide alkyne cycloaddition), DHB (2,5-dihydroxybenzoic acid), DIPEA (*N,N'*-diisopropylethylamine), HCCA (α-cyano-4-hydroxycinnamic acid), TBTA (tris[(1-benzyl-1*H*-1,2,3-triazol-4-yl)methyl]amine), TFA (trifluoroacetic acid), THF (tetrahydrofuran). Compounds **4** [23], **7** [18] and **8** [18] were previously synthesized in our group. Tetrabromobenzene **3** is commercially available.

2.2 Synthesis

Synthesis of 1,2,4,5-tetrakis((trimethylsilyl)ethynyl)benzene 5 [24]

Tetrabromobenzene **3** (158 mg, 0.40 mmol) was dissolved under nitrogen atmosphere with distilled Et_2NH (2 mL) and $(Ph_3P)_2PdCl_2$ (7.1 mg, 0.010 mmol), CuI (1.0 mg, 0.005 mmol), ethynyltrimethylsilane (270 μL, 1.92 mmol) were added in the order. The reaction was stirred at 50 °C for 19 h, TLC analysis showed complete conversion (eluent: *n*-hexane, R_f = 0.08). The mixture was filtered over a celite pad and washed with Et_2O. Evaporation of the solvent afforded crude **5** that was pure enough to be used in the next synthetic step without further purification. The spectroscopic data are in accordance with those previously reported in the literature.

^{1}H NMR (400 MHz, $CDCl_3$) δ (ppm): 7.56 (s, 2 H), 0.25 (s, 36 H).

MS (ESI) *m*/*z*: calcd for $C_{26}H_{38}Si_4$ 462.20; found 485.08 $[M+Na]^+$.

Synthesis of 1,2,4,5-tetraethynyl benzene 5a [24]

Crude **5** (50.6 mg, 0.109 mmol) was dissolved under nitrogen atmosphere in dry CH_2Cl_2 (900 μL). Then a NaOH solution in MeOH (45.2 mg in 700 μL) was added and the reaction was stirred at room temperature for 5 h, monitoring by TLC (eluent: *n*-hexane - EtOAc, 20:1, R_f = 0.33). The solvent was evaporated, the crude was dissolved in CH_2Cl_2 (5 mL) and filtered washing with fresh CH_2Cl_2 (5 mL) to remove a white precipitate. The organic phase was washed with brine (2x5 mL) and dried over anhydrous Na_2SO_4. Evaporation of the solvent afforded crude **5a** that was pure enough to be used in the next synthetic step without further purification. The spectroscopic data are in accordance with those previously reported in the literature.

^{1}H NMR (400 MHz, $CDCl_3$) δ (ppm): 7.64 (s, 2 H), 3.42 (s, 4 H).

MS (EI) *m*/*z*: calcd for $C_{14}H_6$ 174; found 174 $[M]^{+\cdot}$.

Synthesis of compound 6

Crude **5a** (2.7 mg, 0.012 mmol) was dissolved under nitrogen atmosphere in dry THF (70 μL) and $(Ph_3P)_2PdCl_2$ (1.3 mg, 0.002 mmol), CuI (1.5 mg, 0.008 mmol), distilled DIPEA (12 μL, 0.069 mmol) were added in the order. Finally, the aryl iodide **4** (40 mg, 0.068) was added as a solution in dry THF (84 μL). The reaction was stirred at 50 °C for 3 h and complete conversion was assessed by TLC analysis (eluent: CH_2Cl_2 - MeOH, 9:1, R_f = 0.61) monitoring at 365 nm. The solvent was evaporated and the product isolated by flash chromatography (eluent: CH_2Cl_2 - MeOH, 20:1 for 6 fractions then CH_2Cl_2 - MeOH, 15:1). A further purification was performed by size-exclusion chromatography using a Sephadex LH-20 column (Ø = 3 cm, height = 50 cm; eluent: MeOH) affording pure **6** (7.4 mg, 30% over three steps from **3**).

^{1}H NMR (400 MHz, $CDCl_3$) δ (ppm): 7.77 (s, 2 H), 7.02 (s, 4 H), 7.00 (s, 4 H), 4.18 (t, *J* = 4.6 Hz, 8 H), 3.98 (t, *J* = 4.6 Hz, 8 H), 3.83-3.78 (m, 16 H), 3.72-3.68 (m, 16 H), 3.66-3.61 (m, 16 H), 1.14 (s, 84 H).

^{13}C NMR (100 MHz, $CDCl_3$) δ (ppm): 154.4 (C), 153.6 (C), 134.7 (CH), 125.6 (C), 119.3 (CH), 117.6 (CH), 115.2 (C), 114.3 (C), 102.5 (C), 98.0 (C), 93.2 (C), 92.2 (C), 73.1 (2xCH_2), 70.3 (CH_2), 69.7 (2xCH_2), 69.2 (CH_2), 62.0 (CH_2), 61.9 (CH_2), 18.9 (CH_3), 11.5 (C).

MS (ESI) *m*/*z*: calcd for $C_{114}H_{166}O_{24}Si_4$ 2032.09; found 700.3 $[M+3Na]^{3+}$, 1038.93 $[M+2Na]^{2+}$, 2054.88 $[M+Na]^+$.

MS (MALDI) *m*/*z*: calcd for $C_{114}H_{166}O_{24}Si_4$ 2032.1; found 2056.1 $[M+Na]^+$ (matrix DHB).

Synthesis of compound C1

The tetravalent cross-shaped scaffold **6** (5.3 mg, 2.6 μmol) was dissolved in freshly distilled THF (105 μL) under nitrogen atmosphere. Bu_4NF (10 μL) was added as a 1 M solution in THF and the reaction was stirred at room temperature for 1 h. Complete deprotection was assessed by TLC analysis (eluent: CH_2Cl_2 - MeOH, 9:1, R_f = 0.29) monitoring at 365 nm. A solution of TBTA (280 μg, 0.53 μmol) in freshly distilled THF (38 μL) was added, followed by 13 μL of a solution of $CuSO_4 \cdot 5\ H_2O$ (60 μg, 0.24 μmol) and 17 μL of a solution of sodium ascorbate (210 μg, 1.06 μmol) both in degassed H_2O (purged with nitrogen). Finally, dendron **7** (20 mg, 11.4 μmol) was added followed by THF (94 μL) and H_2O (102 μL) to reach a ~ 2:1 THF/H_2O mixture. The reaction was stirred at room temperature, under nitrogen atmosphere, shielded from light for 15 h. The complete conversion into the desired product was assessed by TLC analysis (eluent: CH_2Cl_2 - MeOH, 7:3 + 0.5 H_2O, R_f = 0.22) monitoring at 365 nm and by MALDI-TOF MS (matrix DHB, HCCA). The copper scavenger QuadraSil MP was added to the solution which was stirred for 15 min. After filtering, the crude was finally purified by size-exclusion chromatography using a Sephadex LH-20 column (Ø = 3 cm, height = 50 cm; eluent: MeOH) and monitoring by TLC (eluent: CH_2Cl_2- MeOH, 7:3 + 0.5 H_2O). Dendrimer **C1** was recovered as a bright yellow oil (20.3 mg, 92%). The purity was confirmed by HPLC analysis of an analytical sample by a Waters Atlantis T3 5 μm 4.6x100 mm column, plateau at 90% (H_2O + 0.1% TFA) – 10% (CH_3CN + 0.1% TFA) for 1 min followed by a gradient to 100% (CH_3CN + 0.1% TFA) in 10 min, followed by a plateau for 1 min, flow rate 1 mL/min, λ = 254 nm, t_R (product) = 7.0 min. $[\alpha]_D^{16}$ = + 28.5 (*c* = 0.49 in MeOH).

^{1}H NMR (600 MHz, D_2O) δ (ppm): 8.39 (bs, 4 H), 7.94 (s, 12 H), 7.80 (bs, 2 H), 7.73 (bs, 4 H), 7.07 (bs, 4 H), 4.96 (s, 12 H), 4.59 (bs, 32 H), 4.46 (bs, 24 H), 4.28 (bs, 8 H), 4.04-3.91 (m, 52 H), 3.90-3.83 (m, 44 H), 3.81 (dd, *J* = 9.5, 3.1 Hz, 12 H), 3.76-3.72 (m, 20 H), 3.72-3.62 (m, 120 H), 3.62-3.57 (m, 20 H), 3.55 (bs, 8 H), 3.49 (bs, 8 H), 3.38-3.21 (m, 32 H), 2.82 (td, *J* = 12.1, 3.0 Hz, 12 H), 2.46 (td, *J* = 12.1, 2.7 Hz, 12 H), 1.96 (t, *J* = 14.0 Hz, 24 H), 1.73 (t, *J* = 13.2 Hz, 12 H), 1.45 (t, *J* = 13.2 Hz, 12 H).

^{13}C NMR (100 MHz, D_2O) δ (ppm): 176.9 (C), 176.6 (C), 153.7 (C), 148.7 (C), 144.4 (C), 141.6 (C), 135.0 (CH), 125.8 (C), 125.6 (CH), 125.0 (CH), 120.9 (C), 117.4 (CH), 112.2 (C), 111.8 (CH), 98.8 (CH), 92.5 (C), 84.8 (C), 74.3 (CH), 73.4 (CH), 72.6 (CH_2), 71.8 (CH_2), 70.9 (2xCH), 70.7 (CH), 70.6 (CH), 69,8 (3xCH_2), 69,4 (CH_2), 68.8 (CH_2), 68.1 (4xCH_2), 66.8 (CH), 66.7 (CH_2), 63.7 (CH_2), 61.0 (CH_2), 60.6 (2xCH_2), 52.6 (2xCH_3), 50.1 (2xCH_2), 44.9 (C), 38.7 (2xCH), 27.2 (CH_2), 26.2 (CH_2).

HRMS (ESI) *m*/*z*: calcd for $C_{366}H_{534}N_{48}O_{176}$ 8421.44331; found 1426.56540 $[M+6Na]^{6+}$, 1707.28033 $[M+5Na]^{5+}$, 1711.67260 $[M-H+6Na]^{5+}$, 2128.36951 $[M+4Na]^{4+}$, 8421.46951 by deconvolution.

Synthesis of compound C2

The tetravalent cross-shaped scaffold **6** (4.1 mg, 2.0 μmol) was dissolved in freshly distilled THF (80 μL) under nitrogen atmosphere. Bu_4NF (7.7 μL) was added as a 1 M solution in THF and the reaction was stirred at room temperature for 1 h. Complete deprotection was assessed by TLC analysis (eluent: CH_2Cl_2 - MeOH, 9:1, R_f = 0.29) monitoring at 365 nm. A solution of TBTA (215 μg, 0.41 μmol) in freshly distilled THF (29 μL) was added, followed by 10 μL of a solution of $CuSO_4 \cdot 5\ H_2O$ (60 μg, 0.24 μmol) and 13 μL of a solution of sodium ascorbate (210 μg, 1.06 μmol) both in degassed H_2O (purged with nitrogen). Finally, dendron **8** (21 mg, 8.7 μmol) was added followed by THF (72 μL) and H_2O (78 μL) to reach a ~ 2:1 THF/H_2O mixture. The reaction was stirred at room temperature, under nitrogen atmosphere, shielded from light for 5 days. The complete conversion into the desired product was assessed HPLC analysis. The copper scavenger QuadraSil MP was added to the

solution which was stirred for 15 min. After filtering, the crude was finally purified by size-exclusion chromatography using a Sephadex LH-20 column (Ø = 3 cm, height = 50 cm; eluent: MeOH) and monitoring by TLC (eluent: CH_2Cl_2 - MeOH, 7:3 + 0.5 H_2O). Dendrimer **C2** was recovered as a bright yellow oil (15 mg, 70%). The purity was confirmed by HPLC analysis of an analytical sample by a Waters Atlantis T3 5 μm 4.6x100 mm column, plateau at 90% (H_2O + 0.1% TFA) – 10% (CH_3CN + 0.1% TFA) for 1 min followed by a gradient to 100% (CH_3CN + 0.1% TFA) in 15 min, followed by a plateau for 2 min, flow rate 1 mL/min, λ = 254 nm, t_R (product) = 8.0 min.

^{1}H NMR (600 MHz, $(CD_3)_2SO$) δ (ppm): 8.49 (bs, 4 H), 8.30 (bt, *J* = 5.6 Hz, 12 H), 8.21 (bt, *J* = 5.6 Hz, 12 H), 8,02 (s, 12 H), 7.88 (bs, 4 H), 7.81 (bs, 2 H), 7.26 (bs, 4 H), 7.20 (d, *J* = 7.1 Hz, 48 H), 7.14 (t, *J* = 7.8 Hz, 48 H), 5.09 (t, *J* = 5.6 Hz, 24 H), 4.76 (s, 12 H), 4.73 (d, *J* = 2.4 Hz, 12 H), 4.67 (d, *J* = 2.0 Hz, 12 H), 4.58 (d, *J* = 2.7 Hz, 12 H), 4.55-4.47 (m, 44 H), 4.47-4.40 (m, 72 H), 4,23-4.11 (m, 56 H), 4.11-4.02 (m, 8 H), 3.94-3.86 (m, 8 H), 3.87-3-78 (m, 16 H), 3.78-3.68 (m, 52 H), 3.61 (bs, 12 H), 3.56-3.34 (m, 136 H), 3.17 (d, *J* = 4.3 Hz, 8 H), 2.74 (quint., *J* = 12.6 Hz, 24 H), 1.83-1.64 (m, 36 H), 1.59 (t, *J* = 12.2 Hz, 12 H).

^{13}C NMR (150 MHz, $(CD_3)_2SO$) δ (ppm): 174.0 (2xC), 153.7 (C), 148.5 (C), 144.0 (C), 141.0 (C), 140.6 (C), 138.0 (C), 134.4 (CH), 126.6 (2xCH), 126.2 (2xCH), 124.8 (C), 124.7 (CH), 124.1 (CH), 121.9 (C), 117.1 (CH), 111.4 (CH), 111.2 (C), 98.7 (CH), 91.1 (C), 85.5 (C), 74.6 (CH), 74.2 (CH), 72.6 (CH_2), 72.1 (CH_2), 70.9 (CH), 70.5 (CH), 70.4 (CH), 69.3 (CH_2), 69.1 (2xCH_2), 68.8 (2xCH_2), 68.6 (2xCH_2), 67.8 (2xCH_2), 67.0 (CH), 66.5 (CH_2), 64.0 (CH_2), 62.6 (CH_2), 61.3 (CH_2), 60.2 (2xCH_2), 49.3 (2xCH_2), 44.9 (C), 41.5 (2xCH_2), 39.5 (2xCH), 28.2 (CH_2), 27.8 (CH_2).

HRMS (ESI) *m*/*z*: calcd for $C_{534}H_{702}N_{72}O_{176}$ 10944.83778; found 1847.13142 $[M+6Na]^{6+}$, 2211.96258 $[M+5Na]^{5+}$, 10944.85366 by deconvolution.

2.3. Surface Plasmon Resonance analysis

All the direct interaction experiments were executed on a T200 Biacore with a CM3 series S sensor chip. DC-SIGN and langerin extracellular domains harboured a StreptagII in their *N*-terminus (DC-SIGN S-ECD and langerin S-ECD) to allow their capture and functionalization onto the surface in an oriented manner. Flow cells were functionalized as previously described [25]. Briefly, after EDC/NHS activation, flow cells were functionalized with streptactin protein in a first step. Flow cell 1 was used as it is as control, while other flow cells were, after a second round of activation, functionalized with 49 μg/mL and 55.9 μg/mL of DC-SIGN S-ECD and langerin S-ECD, respectively, up to a final density ranging between 2000 and 3000 RU, via tag specific capture and linkage by amine coupling chemistry simultaneously. The compounds were injected in running buffer of 25 mM Tris pH 8, 150 mM NaCl, 4 mM $CaCl_2$, 0.05% Tween 20 onto the surface at increasing concentrations with a flow rate of 30 μL/min. The ligand titration led to the determination of an apparent K_D value. The data was analysed in BIAcore BIAevaluation software for steady state affinity calculations assuming that the K_D will reflect the affinity of the ligands (glycoclusters) with the DC-SIGN oriented surface.

3. Results

3.1. Synthesis of cross-shaped glycodendrimers

For the synthesis of glycodendrimers **C1** and **C2**, we identified the tetravalent phenylene-ethynylene core **6** as a key intermediate, which enables for late stage diversification at its four ends through copper catalyzed alkyne azide cycloaddition (CuAAC) (Scheme 1). From a retrosynthetic point of view, the central core **6** can originate from the iodide synthon **4** [23] and the protected tetraalkynylbenzene unit **5**, whose synthesis has been reported starting from 1,2,4,5-tetrabromobenzene **3** [24].

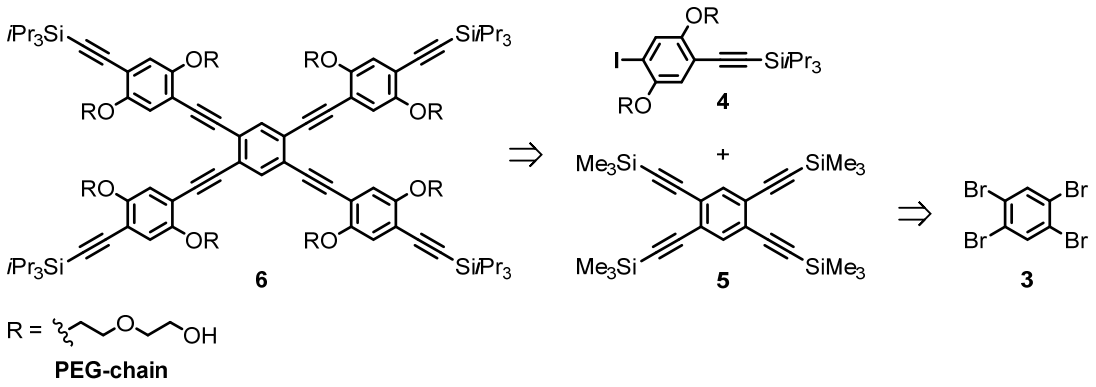

Scheme 1. Retrosynthetic analysis for the preparation of the key intermediate **6**.

As the first step of the synthesis (Scheme 2), a Sonogashira coupling of 1,2,4,5-tetrabromobenzene **3** with trimethylsilylacetylene afforded the desired protected tetraalkynyl **5** as a pure product, which was directly submitted to a deprotection reaction. Removal of the trimethylsilyl groups under basic conditions proceeded smoothly, yielding the tetraalkynyl central unit **5a** with no need of further chromatographic purification. The selective formation of both **5** and **5a** was confirmed by ^{1}H NMR and electron impact (EI) MS analyses. A second Sonogashira coupling enabled connecting the central unit **5a** to four copies of iodide **4** [23], finally providing the protected tetravalent scaffold **6**. The formation of the product was monitored exploiting the intrinsic fluorescence of the construct, which allows its detection by TLC analysis (365 nm irradiation), and by ESI-MS analysis. Purification by flash chromatography followed by a size-exclusion chromatography (Sephadex LH-20 column) afforded the pure core **6** in 30% yield over three steps from **3**.

With the phenylene-ethynylene core **6** in hand, the glycodendrimers **C1,2** were finally accessible (Scheme 2). In situ deprotection of terminal alkyne moieties within **6** was accomplished upon treatment with a Bu_4NF solution in THF for 1 h, and monitored by TLC analysis at 365 nm until full conversion was observed. A subsequent CuAAC step guaranteed efficient functionalization of the rigid tetravalent scaffold with four copies of either azido tethered glycodendrimer **7** or **8** [18]. The reaction progression was assessed either by MALDI-TOF MS (DHB matrix) or HPLC analysis; purification by size-exclusion chromatography (Sephadex LH-20) afforded the final constructs **C1** and **C2** in very good yield (92% and 70% respectively). Pleasantly, the constructs showed good solubility in water (**C1**, 2.5 mM) or water + 4% DMSO solution (**C2**, 0.2 mM); they were fully characterized by NMR and HRMS and their purity was assessed by HPLC analysis.

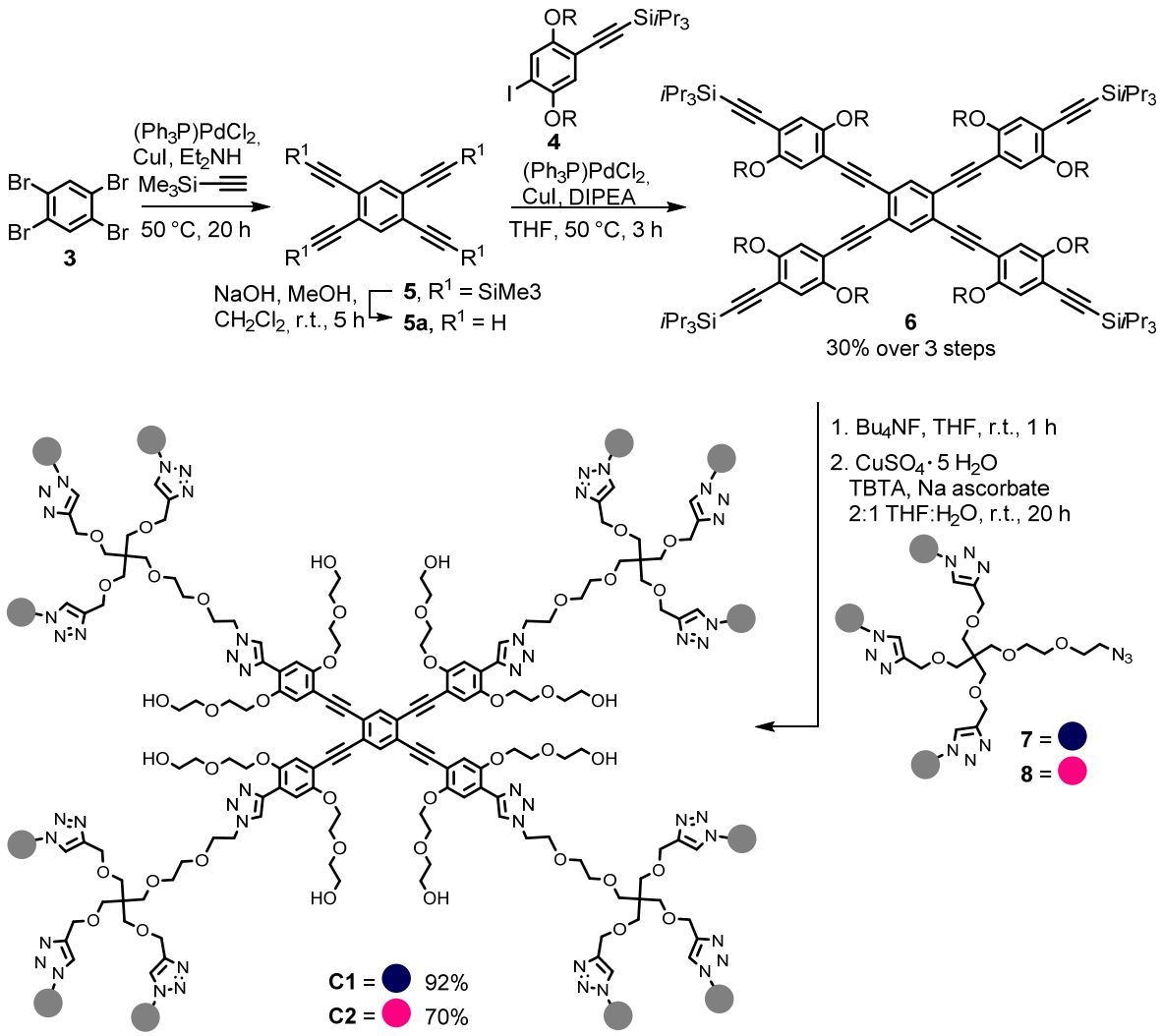

Scheme 2. Synthetic route towards the cross-shaped glycodendrimers **C1,2**.

3.2. Surface plasmon resonance inhibition studies with DC-SIGN

The biological activity of glycodendrimers **C1** and **C2** towards DC-SIGN S-ECD and langerin S-ECD was assessed and compared with the corresponding linear constructs **PM31** and **PM26** by an established Surface Plasmon Resonance (SPR) direct interaction assay [25]. In this test, increasing concentrations of glycodendrimer solutions are flown over the surface of a sensor chip, functionalized with the immobilized targeted C-type lectins. Analysis of the assay sensorgrams provides the corresponding thermodynamic apparent dissociation constants K_D (Table 1 and Figure 3). These tests showed that the glycodendrimers **C1,2** strongly bind to DC-SIGN in comparable way with the previously reported linear **PM31**, **PM26**. The **C1** construct, loaded with 12 copies of the pseudo-1,2-mannobioside ligand **1**, is almost two times more effective than its related hexavalent linear glycoconjugate **PM31** (K_D = 19.0 nM and 32.3 nM respectively). On the other hand, the constructs carrying the more active and selective bis-amide monovalent ligand **2**, i.e. the cross-shaped **C2** and linear **PM26** glycodendrimers, exhibit exactly the same potency (K_D = 10.4 nM and 10.3 nM respectively), corresponding to a lower multivalency enhancement factor (β) for the higher valency **C2**. Direct interaction studies with langerin ECD showed that selectivity depends mostly on the nature of the monovalent ligand: both the **PM26** and **C2** constructs loaded with the intrinsically DC-SIGN selective ligand **2** discriminate effectively against langerin and for DC-SIGN. However, interestingly, the introduction of the tetravalent core within the dendrimer scaffold translates into an increased selectivity towards DC-SIGN, with **C2** reaching a factor of 15.0.

Table 1. Dissociation constants K_D of glycodendrimers **PM31**, **PM26** and **C1,2** obtained for direct interaction with DC-SIGN and Langerin by SPR assays.

Dendrimer	K_D (nM)		*S*
	DC-SIGN	Langerin	
PM31	32.3	55.9	1.7
C1	19.0	41.9	2.2
PM26	10.3	107	10.4
C2	10.4	157	15.0

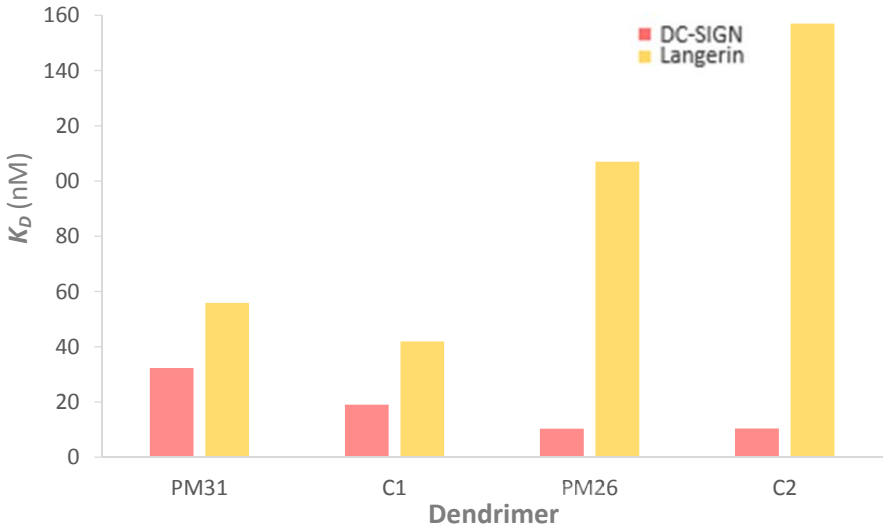

Figure 3. Comparison of dissociation constant K_D values of glycodendrimers **PM31**, **PM26** and **C1,2** towards DC-SIGN (red bar) and langerin (yellow bar) obtained by direct interaction SPR assay. The intrinsic activity of the monovalent ligands **1** and **2**, estimated by binding inhibition assays (SPR) are 0.9 and 0.3 mM, respectively [10].

4. Discussion

The early involvement of DC-SIGN in the setting of viral infections makes it a promising target in the development of antiadhesive drugs. Most of the antagonists developed so far interact with DC-SIGN by mimicking the highly mannosylated structure of the natural occurring $(Man)_9(GlcNAc)_2$ (Man_9) ligand, which is often exposed in multiple presentation by several pathogenic proteins.

During the past years, we have disclosed multivalent presentations of glycomimetics as a successful strategy to access potent and selective DC-SIGN antagonists. Our endeavors have led to the pseudo-1,2-dimannobiosides **1,2**, which mimic the Manα(1,2)Man terminal epitopes of Man_9, featuring increased potency, improved drug-like properties and higher stability towards glycosidases. Both mimics have been obtained replacing the reducing end mannose of the Manα(1,2)Man unit by a conformationally locked cyclohexanediol ring, with the bis-amido derivative **2** performing as the most potent and selective of the series [10,19]. Multivalent presentation of mimics **1,2** with glycodendrimers was crucial to achieve high levels of avidity [18], which was boosted when the glycomimetics were loaded on the linear rigid **PM31**, **PM26** dendrimers, specifically tailored to enable chelation of contiguous CRDs within the DC-SIGN tetramer [11].

Herein we have presented the structurally related cross-shaped glycodendrimers **C1,2**, which are extended enough to simultaneously reach the four CRDs of DC-SIGN. Key for the preparation of

the constructs was the synthesis of the four arms intermediate **6**, which was readily accessed by a streamlined route from tetrabromobenzene **3**. The four protected terminal alkynes moieties of **6** give a handle to functionalize the scaffold in a modular fashion and to obtain **C1,2** through a straightforward one-pot deprotection-CuAAC sequence.

The role of the phenylene-ethynylene core of glycodendrimers **C1,2** is of crucial importance. The rigidity and planarity of the structure concurrently favor binding by determining preorganization of the ligands, while decreasing the overall entropy of the system. Of equal importance is the presence of polyethylene glycol (PEG) chains appended to the core, which allows the dendrimers to be soluble in water solutions, a fundamental requirement for a possible use as therapeutic agents.

Direct interaction studies with DC-SIGN performed by SPR assay revealed that both **C1** and **C2** act as potent antagonists, binding DC-SIGN with nanomolar activity (K_D = 19.0 nM and 10.4 nM respectively). As expected, higher potency was shown by dendrimer **C2**, bearing multiple copies of the most performing monovalent bis-amido ligand **2**. However, the increased valency of the cross-shaped **C1,2** is not reflected in a significant gain of avidity, as confirmed by comparing the K_D of these constructs with those of the respective previously developed linear **PM31**, **PM26**. This observation suggests that while multivalent effects, comprising chelation of adjacent CRDs, are still operative, simultaneous coordination of the four CRDs of DC-SIGN may not be occurring, or may not have a significant effect in reducing the dissociation constant of the complex. The relative selectivity towards DC-SIGN was assessed by analogous SPR direct interaction studies with langerin, a transmembrane C-type lectin showing affinities for mannose, but characterized by an homotrimeric structure, with the CRDs exposed in a trefoil presentation with binding sites separated by 4.2 nm [26]. Remarkably, these tests highlighted that, despite the modest contribution to potency, the tetravalent rigid core positively affects the relative selectivity (S) of the dendrimers (S = 2.2 and 15.0 respectively). The enhanced selectivity might possibly arise from the squared arrangement of the ligands imparted by the rigid planar core of the dendrimers, which may disfavor the binding towards C-type lectins with different geometrical display of the CRDs. The high degree of selectivity observed for glycodendrimers **C2** and **PM26**, bearing multiple copies of the pseudo-dimannobioside **2**, is ascribed to the lower affinity of this monovalent ligand for langerin compared to the pseudo-1,2-mannobioside **1** [10].

5. Conclusions

We were able to study the interaction between DC-SIGN and two glycodendrimer antagonists possessing the structural requirements to simultaneously reach the four CRDs exposed by the target lectin. The novel constructs are characterized by a rigid cross-shaped scaffold, which pre-organizes and directs the ligands to fit the CRDs arrangement of DC-SIGN, and by the presence of PEG pendants, which confer water solubility to the dendrimers. This central property allowed to evaluate the biological activity of the dendrimers by SPR assay, which demonstrated that both **C1** and **C2** act as potent antagonists of DC-SIGN. The results suggest that while the constructs are probably able to chelate two adjacent CRDs, a fine tuning for a better compromise between rigidity and flexibility is likely necessary to accomplish a tetracoordination of the tetramer. Importantly, the improved selectivity displayed by the cross-shaped glycodendrimers **C1,2**, compared to linear analogs **RPM31**, **PM26**, confirm structure-based design as a powerful approach for the planning and development of multivalent antagonists with increased DC-SIGN targeting. Finally, straightness and modularity are remarkable characteristic of the synthetic route that we adopted. Analogous elaboration of scaffolds with proper geometry could enable the generation of multivalent antagonists selective for a variety of pattern-recognizing receptors.

Author Contributions: Conceptualization and methodology, A.B., F.F.; investigation, G.G., C.C., C.V. and S.A.; writing—original draft preparation G.G. and A.B.

Funding: This work was supported by a doctoral fellowship from MIUR (G.G.), by a Marie Curie Outgoing Fellowship to (C.C.) under REA grant agreement no. PIOF-GA-2012-327579 and by the European Union's

Horizon 2020 research and innovation program under the Marie Sklowdowska-Curie grant agreement No. 642870 (Immunoshape) (S.A.).

The Multistep Protein Purification Platform (MP3) was exploited for human DC-SIGN and langerin S-ECD production and the SPR platform for the direct interaction tests of the Grenoble Instruct center (ISBG; UMS 3518 CNRS-CEA-UJF-EMBL) with support from FRISBI (ANR-10-INSB-05-02) and GRAL (ANR-10-LABX-49-01) within the Grenoble Partnership for Structural Biology.

Acknowledgments: We thank Gabriele Conti for technical help with the synthesis of intermediate **6**. This work used the UNITECH- COSPECT platform for MS analysis at the University of Milan.

Conflicts of Interest: The authors declare no conflict of interest.

References

1. Bertozzi, C.R.; Kiessling, L. L. Chemical glycobiology. *Science* **2011**, *291*, 2357-2364. DOI: 10.1126/science.1059820.
2. Mammen, M.; Choi, S.-K.; Whitesides, G. M. Polyvalent interactions in biological systems: implications for design and use of multivalent ligands and inhibitors. *Angew. Chem. Int. Ed.* **1998**, *37*, 2754-2794. DOI: 10.1002/(SICI)1521-3773(19981102)37:20<2754::AID-ANIE2754>3.0.CO;2-3.
3. Fasting, C.; Schalley, C. A.; Weber, M.; Seitz, O.; Hecht, S.; Koksch, B.; Dernedde, J.; Graf, C.; Knapp, E.-W; Haag, R. Multivalency as a chemical organization and action principle. *Angew. Chem. Int. Ed.* **2012**, *51*, 10472-10498. DOI: 10.1002/anie.201201114.
4. Pieters, R. J. Maximising multivalency effects in protein–carbohydrate interactions. *Org. Biomol. Chem.* **2009**, *7*, 2013-2025. DOI: 10.1039/B901828J.
5. Hudak, J. E.; Bertozzi, C. R. Glycotherapy: New advances inspire a reemergence of glycans in medicine. *Chemistry and Biology* **2014**, *21*, 16-37. DOI: 10.1016/j.chembiol.2013.09.010.
6. Jiménez Blanco, J. L.; Ortiz Melleta, C; García Fernández, J. M. Multivalency in heterogeneous glycoenvironments: hetero-glycoclusters, -glycopolymers and -glycoassemblies. *Chem. Soc. Rev.* **2013**, *42*, 4518-4531. DOI: 10.1039/c2cs35219b.
7. Bernardi, A.; Jiménez-Barbero, J.; Casnati, A.; De Castro, C.; Darbre, T.; Fieschi, F.; Finne, J.; Funken, H.; Jaeger, K.-E.; Lahmann, M.; Lindhorst, T. K.; Marradi, M.; Messner, P.; Molinaro, A.; Murphy, P. V.; Nativi, C.; Oscarson, S.; Penadés, S.; Peri, F.; Pieters, R. J.; Renaudet, O.; Reymond, J.-L.; Richichi, B.; Rojo, J.; Sansone, F. ; Schäffer, C.; Turnbull, W. B.; Velasco-Torrijos, T.; Vidal, S.; Vincent, S.; Wennekes, T.; Zuilhofxy, H.; Imberty, A. Multivalent glycoconjugates as anti-pathogenic agents. *Chem. Soc. Rev.* **2013**, *42*, 4709-4727. DOI: 10.1039/C2CS35408J.
8. Cecioni, S.; Imberty, A.; Vidal, S. Glycomimetics versus multivalent glycoconjugates for the design of high affinity lectin ligands. *Chem. Rev.* **2015**, *115*, 525-561. DOI: 10.1021/cr500303t.
9. Sattin, S.; Bernardi, A. Glycoconjugates and glycomimetics as microbial anti-adhesives. *Trends in Biotechnology* **2016**, *34*, 483-495. DOI: 10.1016/j.tibtech.2016.01.004 4.
10. Varga, N.; Sutkeviciute, I.; Guzzi, C.; McGeagh, J.; Petit-Haertlein, I.; Gugliotta, S.; Weiser, J.; Angulo, J.; Fieschi, F.; Bernardi, A. Selective targeting of Dendritic Cell-Specific Intercellular AdhesionMolecule-3-Grabbing Nonintegrin (DC-SIGN) with mannose-basedglycomimetics: synthesis and interaction studies of bis(benzylamide)derivatives of a pseudomannobioside. *Chem. Eur. J.* **2013**, *19*, 4786-4797. DOI: 10.1002/chem.201202764.
11. Ordanini, S.; Varga, N.; Porkolab, V.; Thépaut, M.; Belvisi, L.; Bertaglia, A.; Palmioli, A.; Berzi, A.; Trabattoni, D.; Clerici, M.; Fieschi, F.; Bernardi, A. Designing nanomolar antagonists of DC-SIGN-mediated HIV infection: ligand presentation using molecular rods. *Chem. Commun.* **2015**, *51*, 3816-3819. DOI: 10.1039/C4CC09709B.
12. Ordanini, S.; Goti, G.; Bernardi, A. From optimized monovalent ligands to size-controlled dendrimers: an efficient strategy towards high-activity DC-SIGN antagonists. *Can. J. Chem.* **2017**, *95*, 881-890. DOI: 10.1139/cjc-2017-0138.
13. Porkolab, V.; Chabrol, E.; Varga, N.; Ordanini, S.; Sutkevičiūtė, I.; Thépaut, M.; García-Jiménez, M. J.; Girard, E.; Nieto, P. M.; Bernardi, A.; Fieschi, F. Rational-differential design of highly specific glycomimetic ligands: targeting DC-SIGN and excluding langerin recognition. *ACS Chem. Biol.* **2018**, *13*, 600–608. DOI: 10.1021/acschembio.7b00958.

14. Geijtenbeek, T. B. H.; Kwon, D. S.; Torensma, R.; van Vliet, S. J.; van Duijnhoven, G. C. F.; Middel, J.; Cornelissen, I. L. M. H. A.; Nottet, H. S. L. M.; KewalRamani, V. N.; Littman, D. R.; Figdor, C. G.; van Kooyk, Y. DC-SIGN, a dendritic cell–specific HIV-1-binding protein that enhances *trans*-infection of T cells. *Cell* **2000**, *100*, 587-597. DOI: 10.1016/S0092-8674(00)80694-7.
15. van Kooyk, Y.; Engering, A.; Lekkerkerker, A. N.; Ludwig, I. S.; Geijtenbeek, T. B. H. Pathogens use carbohydrates to escape immunity induced by dendritic cells. *Curr. Opin. Immunol.* **2004**, *16*, 488-493. DOI: 10.1016/j.coi.2004.05.010
16. Ordanini, S.; Zanchetta, G.; Porkolab, V.; Ebel, C.; Fieschi, F.; Guzzetti, I.; Potenza, D.; Palmioli, A.; Podlipnik, Č.; Meroni, D.; Bernardi, A. Solution behavior of amphiphilic glycodendrimers with a rod-like core. *Macromol. Biosci.* **2016**, *16*, 896−905. DOI: 10.1002/mabi.201500452.
17. Berzi, A.; Ordanini, S.; Joosten, B.; Trabattoni, D.; Cambi, A.; Bernardi, A.; Clerici, M. Pseudo-mannosylated DC-SIGN ligands as immunomodulants. *Scientific Reports* 2016, 6, 35373. DOI: 10.1038/srep35373.
18. Varga, N.; Sutkevičiūtė, I.; Ribeiro-Viana, R.; Berzi, A.; Ramdasi, R.; Daghetti, A.; Vettoretti, G.; Amara, A.; Clerici, M.; Rojo, J.; Fieschi, F.; Bernardi, A. Identification of a promising multivalent inhibitor of the DC-SIGN dependent uptake of HIV-1 and Dengue virus. *Biomaterials* **2014**, *35*, 4175-4184. DOI: 10.1016/j.biomaterials.2014.01.014.
19. Reina, J. J.; Sattin, S.; Invernizzi, D.; Mari, S.; Martínez-Prats, L.; Tabarani, G.; Fieschi, F.; Delgado, R.; Nieto, P.M.; Rojo, J.; Bernardi, A. 1,2-Mannobioside mimic: synthesis, DC-SIGN interaction by NMR and docking, and antiviral activity. *ChemMedChem* **2007**, *2*, 1030-1036. DOI: 10.1002/cmdc.200700047.
20. This concept has been recently exploited to prepare glycosylated antagonists with selectivity for DC-SIGN over langerin and for langerin over ConA respectively: a) Wen, H.-C.; Lin, C.-H.; Huang, J.-S.; Tsai, C.-L.; Chena, T.-F; Wang, S.-K. Selective targeting of DC-SIGN by controlling the oligomannose pattern on a polyproline tetra-helix macrocycle scaffold. *Chem. Commun.* **2019**, *55*, 9124-9127. DOI: 10.1039/c9cc03124c; b) Neuhaus, K.; Wamhoff, E.-C.; Freichel, T.; Grafmüller, A.; Rademacher, C.; Hartmann, L. Asymmetrically branched precision glycooligomers targeting langerin. *Biomacromolecules* **2019**, *20*, 4088-4095. DOI: 10.1021/acs.biomac.9b00906.
21. de Witte, L.; Nabatov, A.; Pion, M.; Fluitsma, D.; de Jong, M. A. W. P.; de Gruijl, T.; Piguet, V.; van Kooyk, Y.; Geijtenbeek, T. B. H. Langerin is a natural barrier to HIV-1 transmission by Langerhans cells. *Nat. Med.* **2007**, *13*, 367-371. DOI: 10.1038/nm1541.
22. Still, W. C.; Kahn, M.; Mitra, A. Rapid chromatographic technique for preparative separations with moderate resolution. *J. Org. Chem.* **1978**, *43*, 2923-2925. DOI: 10.1021/jo00408a041.
23. Pertici, F.; Varga, N.; van Duijn, A.; Rey-Carrizo, M.; Bernardi, A.; Pieters, R. J. Efficient synthesis of phenylene-ethynylene rods and their use as rigid spacers in divalent inhibitors. *Beilstein J. Org. Chem.* **2013**, *9*, 215–222. DOI: 10.3762/bjoc.9.25.
24. Wang, C.-C; Tsai, H.; Shih, H.-H.; Jeon, S.; Xu, Z.; Williams, D.; Iyer, S.; Sanchez, T. C.; Wang, L.; Cotlet, M.; Wang, H.-L. Synthesis and characterization of ethylene glycol substituted poly(phenylene vinylene) derivatives. *ACS Appl. Mater. Interfaces* **2010**, *2*, 738-747. DOI: 10.1021/am900766s.
25. Porkolab, V.; Pifferi, C.; Sutkeviciute, I.; Ordanini, S.; Taouai, M.; Thepaut, M.; Vivès, C.; Benazza, M.; Bernardi, A.; Renaudet, O.; Fieschi, F. Development of C-type lectin oriented surfaces for high avidity glycoconjugates: towards mimicking multivalent interactions on the cell surface. *Org. Biomol. Chem.* **2020**, *18*, 4763-4772. DOI: 10.1039/d0ob00781a.
26. Feinberg, H.; Powlesland, A. S.; Taylor, M. E.; Weis, W. I. Trimeric structure of langerin. *J. Biol. Chem.* **2010**, *285*, 13285-13293. DOI: 10.1074/jbc.M109.086058.